Vehicle stabilization with torque distribution

Document Version:
Publisher's PDF, also known as Version of Record (includes final page, issue and volume numbers)

Please check the document version of this publication:

• A submitted manuscript is the version of the article upon submission and before peer-review. There can be important differences between the submitted version and the official published version of record. People interested in the research are advised to contact the author for the final version of the publication, or visit the DOI to the publisher's website.
• The final author version and the galley proof are versions of the publication after peer review.
• The final published version features the final layout of the paper including the volume, issue and page numbers.

[Link to publication](#)

Vehicle stabilization with torque distribution

Mark Nievelstein

DCT 2004.107

Traineeship report

Coach(es):   dr.ir. Alex Serrarens
             dr.ir. Igo Besselink

Supervisor: prof. ir. N.J.J. Liebrand

Technische Universiteit Eindhoven
Department Mechanical Engineering
Dynamics and Control Technology Group

Eindhoven, September, 2004

Contents

1 Introduction

Recent developments of new automotive powertrain concepts, like the new *E-four* of the Toyota Estima, give rise to new vehicle stability control concepts. The Toyota Estima, developed by the Toyota Motor Corporation, is fitted with a CVT (THS-C) and a separate motor/generator for the rear wheels. In order to achieve maximal fuel efficiency for different driving conditions different driving modes are possible. For switching between these driving modes a set off wet-multiple disc clutches in combination with a planetary gear arrangement is used.

The new *E-four* full hybrid system creates the possibility to "arbitrarily" distribute the applied drive torque between the front and rear axle. This gave rise to the question whether it is possible to positively influence the vehicle dynamics during cornering with a proper powertrain controller.

The problem definition researched in this report is formulated as follows:
"Can a proper powertrain controller positively influence the vehicle dynamics during cornering."
This problem can be decomposed in the following sub tasks:

- construct a powertrain model suited for simulations

- construct a drivemode controller

- construct a vehicle dynamics model and research the influence of torque distribution

- combine the models and compose a controller

In this report the problem stated above is investigated. In the first section the powertrain is analyzed and the relevant equations for the separate components are derived. In the second section these equations are combined and reduced to formulate a state space model for the powertrain simulation. In the third section a drive mode controller is composed en some simulations are performed to validate the powertrain model. In section four the vehicle dynamics model is constructed and the influence of the torque distribution is analyzed. Finally the conclusions are stated and further research is recommended.

2 Drivetrain of the Toyota Estima

The Toyota Estima is the first hybrid minivan with gasoline/electric hybrid four-wheel drive. The goal of a hybrid vehicle is to increase fuel efficiency without reducing performance.

The Toyota Estima has a series/parallel hybrid system (THS-C), which provides superior fuel efficiency and driving performance. The Toyota Hybrid System with CVT has a gasoline as well as a electric motor. Depending on driving conditions the system either uses the driving power from one of the motors or from both motors. For improved driving performance the Toyota Estima is also equipped with a electric motor/generator for the rear axle. The rear electric motor can also be used for regenerative braking.

To derive the equations of motion of the powertrain, at first the powertrain is analyzed. Because of the inherent simplicity of the rear-wheel drive, only the front-wheel drive will be covered here see Figure: 1.
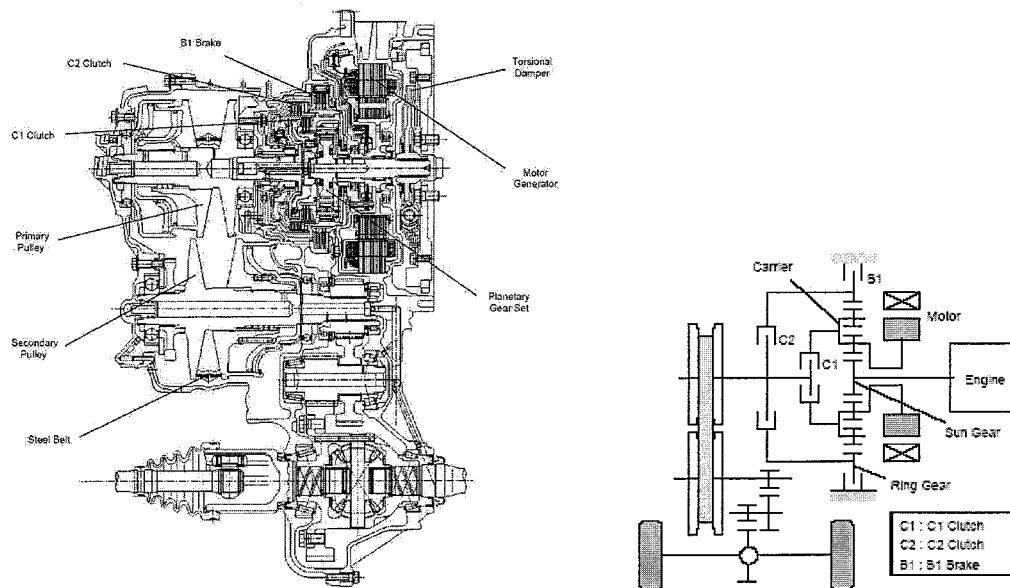

Figure 1: Cross section and schematic of the transaxle [2]

2.1 Equations of motion

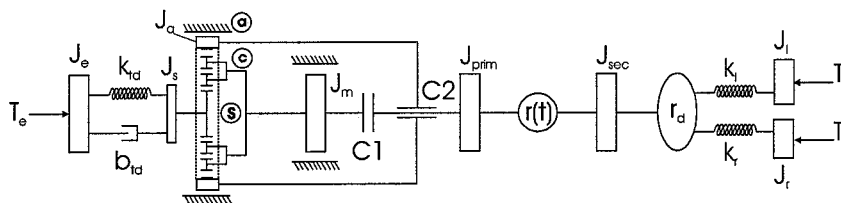First schematic model of the front-wheel drive is composed and shown in Figure 2.

Figure 2: Model of the front drive [4]

The front powertrain is divided into four parts. Parts consist of 1. the Engine, 2. the motor

4

and planetary gear, 3. the CVT, 4. the wheels. The relevant torques, sign conventions and separate parts are defined in Figure 3. Each part contains inertias that are kinematically connected and will be modelled with one or more differential equations. The connections $\mathbf{A}, \mathbf{B}, \mathbf{C}$ between all four parts will be modelled separately by differential or algebraic equations.
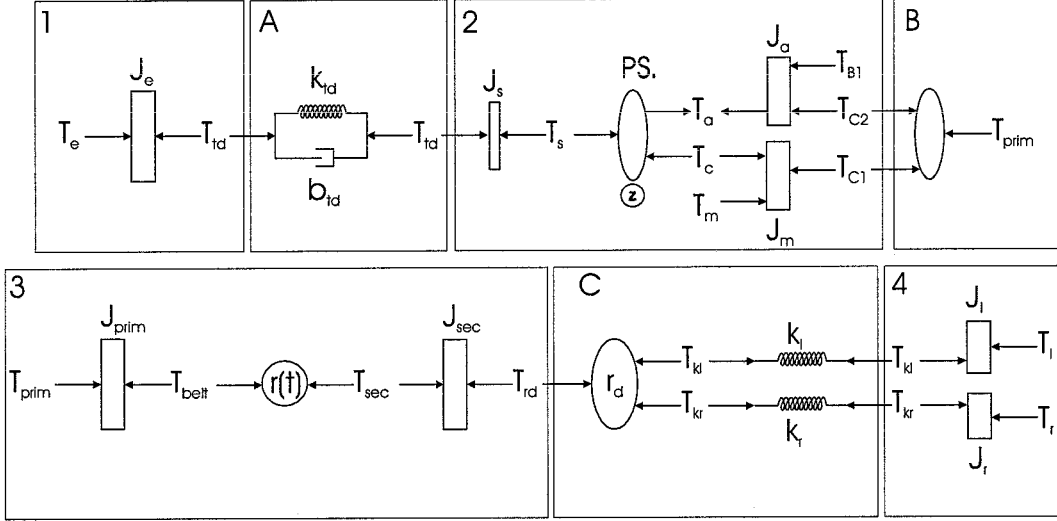

Figure 3: Definitions and sign conventions of the front drive

For obtaining a more expliciet formulation for the total dynamics and reducing the number of differential equations, it is convenient to lump the masses and inertias together where possible. The lumping of inertias is possible if inertias are kinematically linked .

Part 1, the engine

Part 1 only consists of the engine. The engine is modelled as a torque source T_e acting on an inertial weight J_e and a load torque from the torsional damper T_{td}. The resulting equation of motion for this part than becomes:

$$J_e \cdot \dot{\omega}_e = T_e - T_{td} \tag{1}$$

Part A, The torsional damper

The engine is connected to the transmission by means of a torsional damper. The torsional damper is modelled by a linear spring with stiffness k_{td} and a linear damper with dampingconstant b_{td}. The torque transmitted by the torsional damper is T_{td}. Equation (2) describes this connection:

$$\dot{T}_{td} = k_{td} \cdot (\omega_e - \omega_s) + b_{td} \cdot (\dot{\omega}_e - \dot{\omega}_s) \tag{2}$$

Part 2, the planetary gear

The second part consists of a planetary gear and an electric motor. The electric motor is connected to the carrier and their combined inertia is indicated with J_m. The torque from the motor is given by T_m. The torques from the clutches connecting the planetary gear to the CVT are given by T_{C1}, T_{C2} and T_{B1}. The inertia of the sun is represented by J_s and the inertia of the annulus by J_a. The equations of motion for these three gear parts are :

$$J_s \cdot \dot{\omega}_s = T_{td} - T_s \tag{3}$$

$$J_a \cdot \dot{\omega}_a \quad = \quad -T_a - T_{B1} - T_{C2} \tag{4}$$

$$J_m \cdot \dot{\omega}_m \quad = \quad T_c + T_m - T_{C1} \tag{5}$$

The sun annulus and carrier are kinematically coupled, which imposes constraints on equation: (4) to (5). These constraints consist of the kinematic and static equations of the planetary gear. The kinematic equations of a planetary gear with double pinion are [3]:

$$\omega_s = (1 + z) \cdot \omega_c - z \cdot \omega_a \qquad ; z = -\frac{r_a}{r_s} \tag{6}$$

The static equations of a planetary gear are [3]:

$$T_a = z \cdot T_s \tag{7}$$

$$T_c = (1 + z) \cdot T_s \tag{8}$$

To determine the speed op of all the parts of the planetary gear, at least the speeds of two parts need to be know. Hence two differential equations must be solved in order to obtain the third speed. With the use of the links between the equations of motion of the planetary gear, the number of differential equations can be reduced to two equations instead of three.However, first a more general case of a planetary gear with three inertias and three applied torques will be considered. See Figure 4
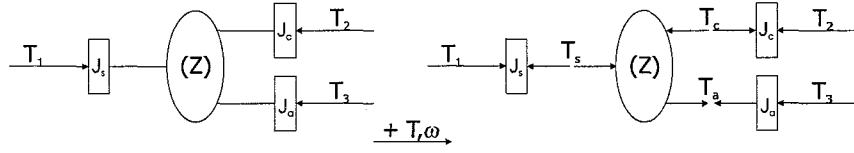
Figure 4: general case of a planetairy gear

The kinematic and static equation for a double pinion planetary gear are (as mentioned above):

$$\omega_s \quad = \quad (1 + z) \cdot \omega_c - z \cdot \omega_a \qquad ; z = -\frac{r_a}{r_s} \tag{9}$$

$$\dot{\omega}_s \quad = \quad (1 + z) \cdot \dot{\omega}_c - z \cdot \dot{\omega}_a \tag{10}$$

$$T_a \quad = \quad z \cdot T_s \tag{11}$$

$$T_c \quad = \quad (1 + z) \cdot T_s \tag{12}$$

The equations of motion for this system are :

$$J_s \cdot \dot{\omega}_s \quad = \quad T_1 - T_s \tag{13}$$

$$J_c \cdot \dot{\omega}_c \quad = \quad T_c - T_2 \tag{14}$$

$$J_a \cdot \dot{\omega}_a \quad = \quad -T_a - T_3 \tag{15}$$

After rewriting and substituting these equations an explicit expression for T_s can be found. This is covered in more detail in appendix B:

$$T_s \quad = \quad \frac{J_a \cdot J_c \cdot T_1 + (1 + z) \cdot J_a \cdot J_s \cdot T_2 - z \cdot J_c \cdot J_a \cdot T_3}{J_c \cdot J_a + J_a \cdot J_s \cdot (1 + z)^2 + J_c \cdot J_s \cdot z^2} \tag{16}$$

6

When applying this to the planetary gear of the Toyota Estima, the equations describing the planetary gear take the following form:

$$\dot{\omega}_s = \frac{T_{td} - T_s}{J_s} \tag{17}$$

$$\dot{\omega}_c = \frac{(1+z) \cdot T_s - (T_{C1} - Tm)}{J_m} \tag{18}$$

$$T_s = \frac{J_a \cdot J_m \cdot T_{td} + (1+z) \cdot J_a \cdot J_s \cdot (T_{C1} - T_m) - z \cdot J_m \cdot J_a \cdot (T_{C2} + T_{B1})}{J_m \cdot J_a + J_a \cdot J_s \cdot (1+z)^2 + J_m \cdot J_s \cdot z^2} \tag{19}$$

With this explicit expression (assuming the applied moments $T_{td}, T_{C1}, T_{C2}, T_{B1}$ and T_m are known) equation. (17) and (18) can be solved. The third speed (ω_a) can be found with use of equation (6). The torques T_c and T_a can be found with the static equations of the planetary gear (7) and (8).

Part B, The clutches, stick / slip

The planetary gear is coupled to the CVT through several clutches. When the clutches are closed further lumping is possible but a different model for each configuration would be necessary. To avoid using different models the clutches are modelled bij the torque they transmit during the slip regime as well as during the stick regime. To calculate the torque transmitted through a clutch the "Karnopp" approach is adopted [6]. The torque which can be transmitted through a locked or slipping clutch depends on the clamping pressure p, the number of plates n, the surface area A, the average radius on which the friction force is applied R and the friction coefficient μ_{stick}.

clutch 1
for clutch 1 the following holds:

$$T_{C1} = \begin{cases} \dfrac{(T_c + T_m) \cdot J_{prim} + (T_{belt} - T_{C2}) \cdot J_m}{J_m + J_{prim}} & \text{if } |\omega_m - \omega_{prim}| < \varepsilon \\[2mm] & \text{and } |T_{C1}| \leq |T_{C1_{stick}}| \\[1mm] n \cdot p \cdot A \cdot R \cdot \mu \cdot sign(\omega_m - \omega_{prim}) & \text{else} \end{cases} \tag{20}$$

$$T_{C1_{stick}} = n \cdot p \cdot A \cdot R \cdot \mu_{stick} \cdot sign(T_{C1}) \tag{21}$$

This is can be derived from figure 5:

Figure 5: Stick/slip system for clutch 1 [4]

Clutch 2
For clutch 2 holds:

$$T_{C2} = \begin{cases} \dfrac{(T_a - T_{B1}) \cdot J_{prim} + (T_{belt} - T_{C1}) \cdot J_a}{J_{prim} + J_a} & \text{if } |\omega_a - \omega_{prim}| < \varepsilon \\[2mm] & \text{and } |T_{C2}| \leq |T_{C2_{stick}}| \\[1mm] n \cdot p \cdot A \cdot R \cdot \mu \cdot sign(\omega_a - \omega_{prim}) & \text{else} \end{cases} \tag{22}$$

$$T_{C2_{stick}} = n \cdot p \cdot A \cdot R \cdot \mu_{stick} \cdot sign(T_{C2}) \tag{23}$$

Figure 6: Stick/slip system for clutch 2 [4]

This is can be derived from figure 6:

Brake 1

And for brake 1 holds:

$$T_{B1} = \begin{cases} T_a & \text{if } |\omega_a - 0| < \varepsilon \wedge |T_{B1}| \leq |T_{B1_{stick}}| \\ n \cdot p \cdot A \cdot R \cdot \mu \cdot sign(\omega_a) & \text{else} \end{cases} \tag{24}$$

$$T_{B1_{stick}} = n \cdot p \cdot A \cdot R \cdot \mu_{stick} \cdot sign(T_{B1}) \tag{25}$$

This is can be derived from figure 7:

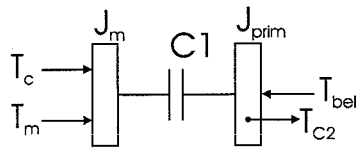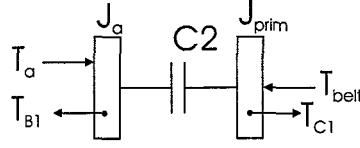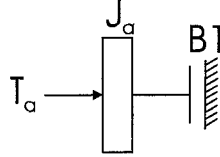Figure 7: Stick/slip system for brake 1 [4]

part 3, CVT

The Continuous Variable Transmission connects the primary shaft to the secondary shaft through a variable ratio. The CVT can be seen as two inertias connected with a time dependant gear ratio and with a primary and secondary torque applied to them, see figure 3. The final-drive inertia is incorporated in the secondary pulley inertia for convenience. The final-drive will be considered to be massless from here on. The equations of motion for the primary and secondary pulleys are:

$$J_{prim} \cdot \dot{\omega}_{prim} = T_{prim} - T_{belt} \tag{26}$$

$$J_{sec} \cdot \dot{\omega}_{sec} = T_{sec} - T_{rd} \tag{27}$$

The kinematic and static equations connecting the pulleys are:

$$\omega_{sec} = \frac{1}{r(t)} \cdot \omega_{prim} \qquad ; r(t) = \frac{\omega_{sec}}{\omega_{prim}} \tag{28}$$

$$T_{belt} = \frac{1}{r(t)} \cdot T_{sec} \tag{29}$$

$$\tag{30}$$

Using these equations the two equations of motion of the CVT pulleys can be reduced to one equation. When lumping two inertias connected by a gear ratio the, the lumped inertia will depend on the gear ratio. If the ratio is time dependant like in a cvt, an extra torque will be induced when the ratio is changed with a speed of $r(t)$ (for convenience the time dependency is not noted in the formulas). Combining the separate EOM and the kinematic relations a combined EOM can be found:

8

$$\dot{\omega}_{prim} \quad = \quad \frac{T_{prim} - \left(\frac{J_{sec} \cdot \omega_{prim} \cdot \dot{r}}{r^3}\right) - \frac{T_{rd}}{r \cdot r_d}}{\left(J_{prim} + \left(\frac{J_{sec}}{r^2}\right)\right)} \tag{31}$$

This is covered in more detail in appendix C. In equation (68) the term $\left(J_{prim} + \left(\frac{J_{sec}}{r^2}\right)\right)$ represents the equivalent inertia of the combined system, and $\left(\frac{J_2 \cdot \omega_{prim} \cdot \dot{r}}{r^3}\right)$ represents the torque induced by the extra acceleration due to continuously variable gear changing.

Part C, The differential

The differential connects the cvt to the wheels. Since the differential is considered to be massless, there are no separate dynamic equations for the differential, but only static and kinematic relations. The kinematic and static equations for a differential are:

$$\omega_{sec} \cdot r_d \quad = \quad \frac{\omega_{dl} + \omega_{dr}}{2} \tag{32}$$

$$T_{r_d} \quad = \quad \frac{1}{r_d} \cdot (T_{k_l} + T_{k_r}) \tag{33}$$

The differential is connected to the wheels by two relatively thin shafts, the driveshafts. The stiffness of these shafts is modelled as followed:

$$\dot{T}_{k_l} \quad = \quad k_l \cdot (\omega_{r_{d_l}} - \omega_l) \tag{34}$$

$$\dot{T}_{k_r} \quad = \quad k_r \cdot (\omega_{r_{d_r}} - \omega_r) \tag{35}$$

Part 4, the wheels

The wheels are considered to be simple inertias with a load torque applied. The EOM for the wheels are:

$$J_l \cdot \dot{\omega}_l \quad = \quad T_{k_l} - T_l \tag{36}$$

$$J_r \cdot \dot{\omega}_r \quad = \quad T_{k_r} - T_r \tag{37}$$

state space

After reducing the number of equations a first order state space model can be formulated. The states are considered to be: $\omega_a, T_{td}, \omega_s, \omega_c, \omega_{prim}, T_{kl}, T_{kr}, \omega_l$ and ω_r. The inputs are considered to be: $T_e, T_m, T_s, T_{C1}, T_{C2}, T_{B1}$ and $\dot{r}$. The model in state space form is given by 38.

$$x \quad = \quad \begin{bmatrix} \omega_a & T_{td} & \omega_s & \omega_c & \omega_{prim} & T_{kl} & T_{kr} & \omega_l & \omega_r & r \end{bmatrix}^T \tag{38}$$

$$u \quad = \quad \begin{bmatrix} T_e & T_m & T_s & T_{C1} & T_{C2} & T_{B1} & T_{loadl} & T_{loadr} & \dot{r} \end{bmatrix}^T \tag{39}$$

$$\tag{40}$$

9

All nonlinearities of the system are incorporated in the algebraic equations needed to calculate the clutch torques. (equations (20),(22) and (24)). T_s can be calculated with equation (19). Now a state space formulation can bo composed of the form:

$$\dot{x} \;=\; f(x) + g(x)u \tag{41}$$

The Matrix $f(x)$ than becomes:

$$
\begin{bmatrix}
\dfrac{-T_{td}}{J_e} \\[4pt]
k_{td} \cdot (\omega_e - \omega_s) + b_{td} \cdot \left(\dfrac{-T_{td}}{J_e} - \dfrac{T_{td}}{J_s} \right) \\[4pt]
\dfrac{T_{td}}{J_s} \\[4pt]
\dfrac{-T_{rd}}{r \cdot r_d \left(J_{prim} + \frac{J_{sec}}{r^2} \cdot \right)} \\[4pt]
k_l \cdot (\omega_{dl} - \omega_l) \\[4pt]
k_r \cdot (\omega_{dr} - \omega_r) \\[4pt]
\dfrac{T_{kl}}{J_l} \\[4pt]
\dfrac{T_{kr}}{J_r} \\[4pt]
0
\end{bmatrix}
\tag{42}
$$

Note that $T_{rd} = T_{kl} + T_{kr}$. And Matrix $g(x)$ becomes:

$$
\begin{bmatrix}
\dfrac{1}{J_e} & 0 & 0 & 0 & 0 & 0 & 0 & 0 & 0 \\[6pt]
\dfrac{b_{td}}{J_e} & 0 & \dfrac{b_{td}}{J_s} & 0 & 0 & 0 & 0 & 0 & 0 \\[6pt]
0 & 0 & \dfrac{-1}{J_s} & 0 & 0 & 0 & 0 & 0 & 0 \\[6pt]
0 & \dfrac{-1}{J_m} & \dfrac{(1+z)}{J_m} & \dfrac{-1}{J_m} & & & & & \\[6pt]
0 & 0 & 0 & \dfrac{1}{\left(J_{prim}+\frac{J_{sec}}{r^2}\right)} & \dfrac{1}{\left(J_{prim}+\frac{J_{sec}}{r^2}\right)} & 0 & 0 & 0 & \dfrac{\left(\frac{J_{sec}\cdot\omega_{prim}}{r^3}\right)}{\left(J_{prim}+\frac{J_{sec}}{r^2}\right)} \\[6pt]
0 & 0 & 0 & 0 & 0 & 0 & 0 & 0 & 0 \\[6pt]
0 & 0 & 0 & 0 & 0 & 0 & \dfrac{-1}{J_l} & 0 & 0 \\[6pt]
0 & 0 & 0 & 0 & 0 & 0 & 0 & \dfrac{-1}{J_r} & 0 \\[6pt]
0 & 0 & 0 & 0 & 0 & 0 & 0 & 0 & 1
\end{bmatrix}
\tag{43}
$$

This state space formulation is modelled in Matlab simulink for simulation purposes.
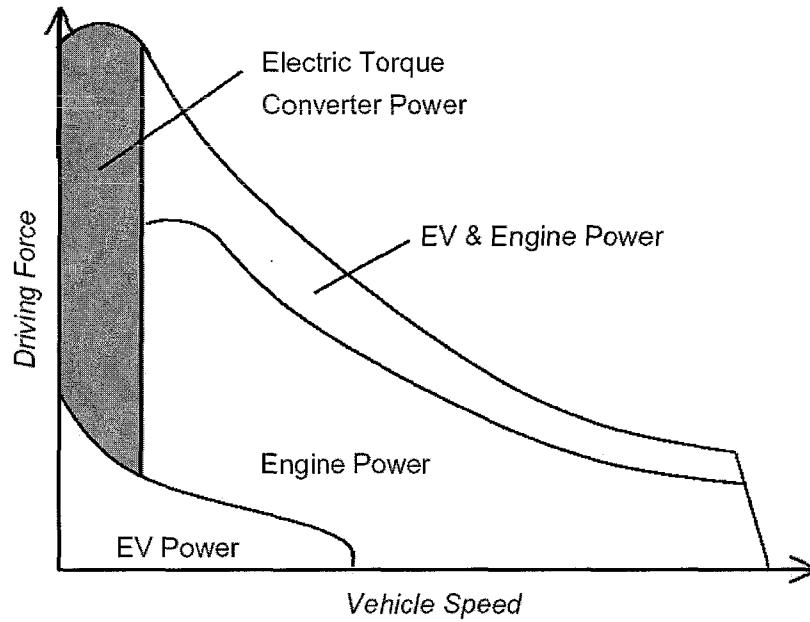
10

2.2 Control strategy

Figure 8: drivemode switchdiagram [2]

The Toyota Estima uses four different D-range driving modes depending on driving conditions and load (fig. 8), to increase efficiency and performance. These modes are:

- EV Power

- Electric Torque Converter Power

- Engine Power

- EV & Engine Power

These different driving modes can be achieves by closing or opening different clutches. See table 1

driving mode	C1	C2	B1
EV power	o		
Engine Power	o	o	
Electric torque converter power		o	
Rev. range[a]	o		Δ
P range charge			o
Nrange			

Table 1: Operation chart of friction elements [2]
o:engage, Δ:Slip
[a]C1: EV power, B1: Engine power (friction mode)

For simulations with the model derived in the previous section drive mode selection is necessary. With use of of the drive mode switch diagram a controller is composed to switch between the drive modes. To ensure smooth switching behavior between drive modes and reduce clutch wear, it is necessary to control the speed of the yet disconnected components. The aim of this speed control is to minimize slip and accompanying torque steps when a clutch is closed. So for each transition incorporating a clutch switch a different control strategy would be necessary. But in order to keep the model as simple as possible only two transitions will be controlled to ensure smooth switching. The remaining transition (between EV power and ETC power) is not considered in this report.

The transition from ETC power to Engine power or EV & Engine power is identical concerning clutch switching is considered. The transition between these modes occurs at a vehicle speed of 21 km/h (v_{ETC}). The engine speed, motor speed and the analus should be the same at this point for smooth switching. When clutch 1 and 2 are both closed the planetary gear is locked. The rotational speed of the planetary gear at a vehicle speed 21 km/h (5.8m/s) can be found with use af the gears connecting them:

$$\omega_{ETC} = r_{cvt} \cdot r_d \cdot \frac{v_{ETC}}{r_{tyre}} \tag{44}$$

If the engine is controlled to maintain a constant speed of $\omega_{ETC} = 215.81[rad/s]$ the speed during the transition for the entire ETC mode, the speed of the motor will always be the same as that of the engine and vehicle when the transition speed is reached.

The transition from EV power to Engine power can be analyzed in a similar way. But now the speed difference for clutch two should be zero. Because there is a wide speed range in which this transition can take place the engine is controlled to match the speed of C2 (ω_a) to the vehicle speed. This is again the lock speed of the planetary gear. So if now the engine speed is controlled to be the same as the motor speed before closing the clutch, there will be minimum slip during the switching of clutch 2.

A hard launch is simulated to illustrate this. During a hard launch the vehicle will start in the ETC mode and switch to the EV & Engine power. The vehicle has an initial speed of 1 km/h and the accelerator is pressed to maximum at $t = 1s$. From this moment the synchronization starts, see fig: 9(c). When the vehicle speed reaches the 21 km/h the speeds are synchronized and the clutch is closed with minimal slip and wear.

The transition from EV power to Engine power can be analyzed in a similar way. But now the speed difference for clutch two should be zero. Because there is a wide speed range in which this transition can take place and fuel economy is not yet considered, the engine is controlled to match the speed of C2 (ω_a) to the primary pulley speed. This is again the lock speed of the planetary gear. So if now the engine speed is controlled to be the same as the motor speed before closing the clutch, there will be minimum slip during the switching of clutch 2. It is impossible for the engine te achieve synchronization below the idle speed of the engine as can be seen in figure 10(c). For speeds above the idle speed, the engine ensures synchronization. At a speed of 25 km/h the torque demand is increased and clutch 2 is closes and the vehicle enters the Engine power mode as can be seen in figure 10(a). The torques transmitted through the clutches after locking of the planetary gearset, becomes $-zT_e$ for C2 and $T_e - T_{C2}$ for C1.
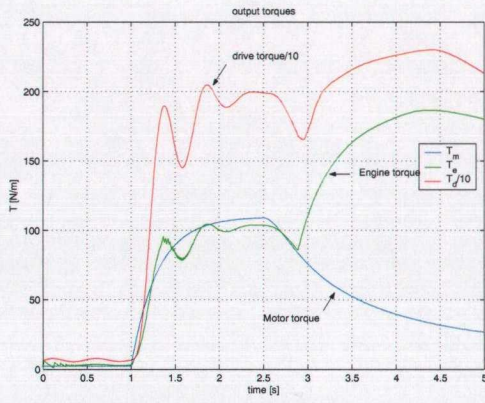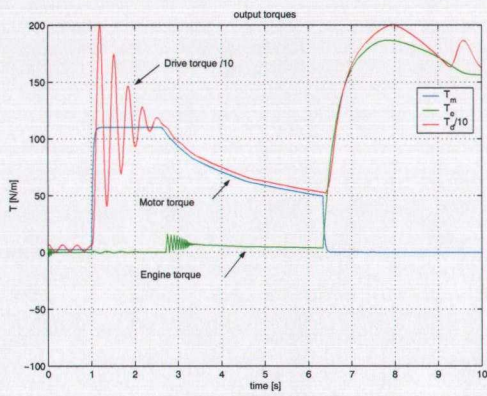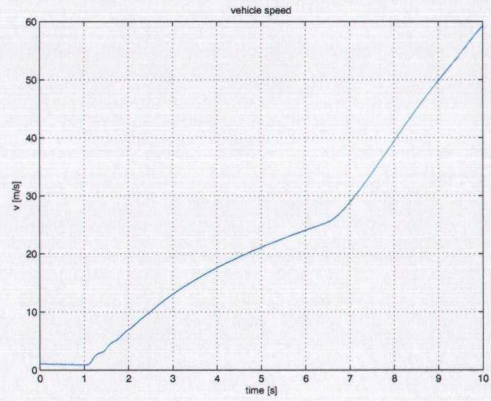
(a) output torques
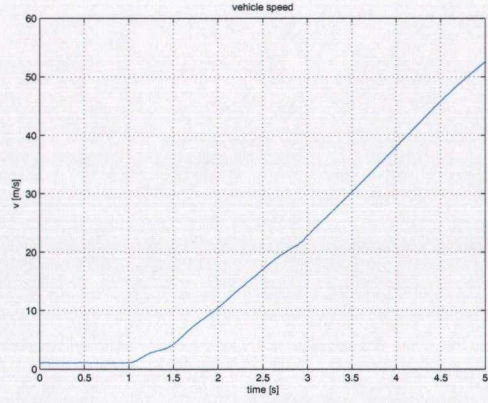
(b) vehicle speed
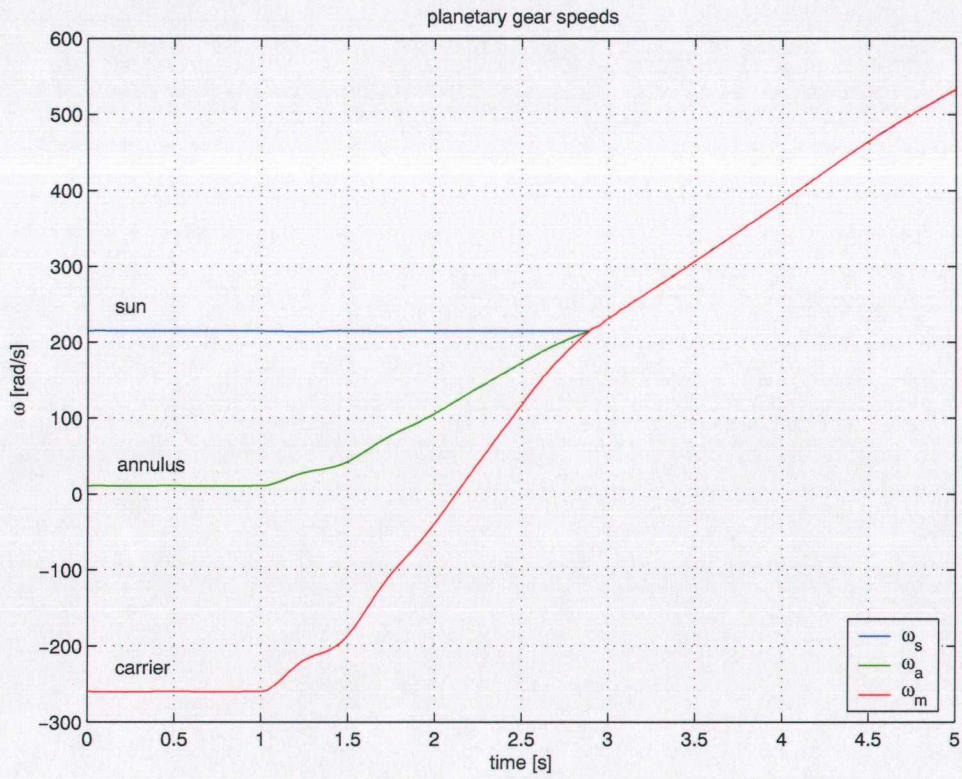
(c) planetary gear speeds
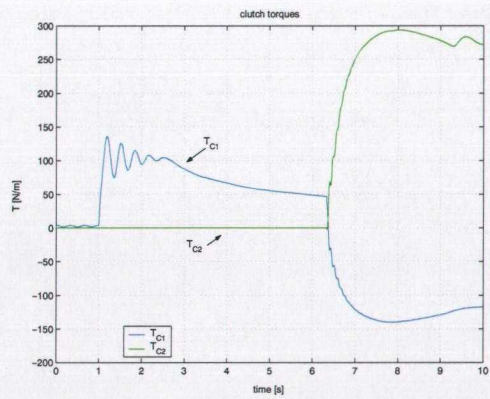
Figure 9: hard launch simulation results

(a) output torques

(b) vehicle speed

(c) planetary gear speeds

(d) clutch torques

Figure 10: EV launch simulation results

14

3 Vehicle dynamics

3.1 Vehicle model

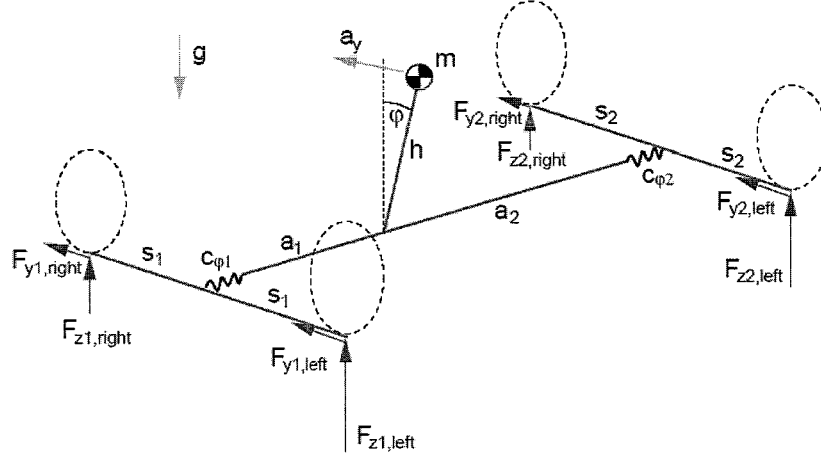In order to analyze the vehicle dynamics a 3D vehicle model has been composed.

Figure 11: Simplified vehicle model [5]

While analyzing the vehicles turning behaviour only constant speed situations are considered, so only lateral accelerations will be considered. The torsional stiffness of the front and rear axle is modeled by a torsional spring located on the road. The vehicle mass is concentrated in a point located at height h and a distance a_1 from the front axle. The difference in side slip angles for the left and right tyres is neglected and thus α_1 is the front axle slip angle and α_2 is the rear axle slip angle. The weight transfer due to lateral acceleration can be derived now and becomes:

$$Fz1r = \frac{m \cdot g \cdot a_2}{(2 \cdot (a_1 + a_2))} - \frac{C_{\phi 1} \cdot a_y \cdot m \cdot h}{(2 \cdot s1 \cdot (C_{\phi 1} + C_{\phi 2} - m \cdot g \cdot h))} \tag{45}$$

$$Fz1l = \frac{m \cdot g \cdot a_2}{(2 \cdot (a_1 + a_2))} + \frac{C_{\phi 1} \cdot a_y \cdot m \cdot h}{(2 \cdot s1 \cdot (C_{\phi 1} + C_{\phi 2} - m \cdot g \cdot h))} \tag{46}$$

$$Fz2r = \frac{m \cdot g \cdot a_1}{(2 \cdot (a_1 + a_2))} - \frac{C_{\phi 2} \cdot a_y \cdot m \cdot h}{(2 \cdot s_2 \cdot (C_{\phi 1} + C_{\phi 2} - m \cdot g \cdot h))} \tag{47}$$

$$Fz2l = \frac{m \cdot g \cdot a_1}{(2 \cdot (a_1 + a_2))} + \frac{C_{\phi 2} \cdot a_y \cdot m \cdot h}{(2 \cdot s_2 \cdot (C_{\phi 1} + C_{\phi 2} - m \cdot g \cdot h))} \tag{48}$$

The first term represents the static weight distribution and the second term represents the weight displacement due to lateral acceleration. In vehicle dynamics the tyre dynamics play an essential role in determining the vehicle behavior. For the evaluation of the forces in the tyre-road contact zone a Magic Formula tyre model is used. To evaluate the Magic Formula a matlab function developed by TNO is used.

To analyse the influence of the E-four on the vehicles turning behavior a handling diagram has been constructed for several torque distributions between front and rear axle see figure 12. This diagram was constructed for a speed of 140 km/h and a roadload of 1150 N. A handling diagram is a means to clearly observe the steady-state handling characteristics of a vehicle. The slope of the vehicle response curves at any point is the negative inverse understeer gradient (-1/K). The neutral steer condition is the infinite slope line of K=0. Understeer vehicles exhibit a negative slope and oversteer vehicles a positive

15

slope on the diagram. On the vertical axis the normalized lateral force is putout. On the horizontal axis the difference between front and rear slip angles is putout. The vehicle parameters are mentioned in figure 12.
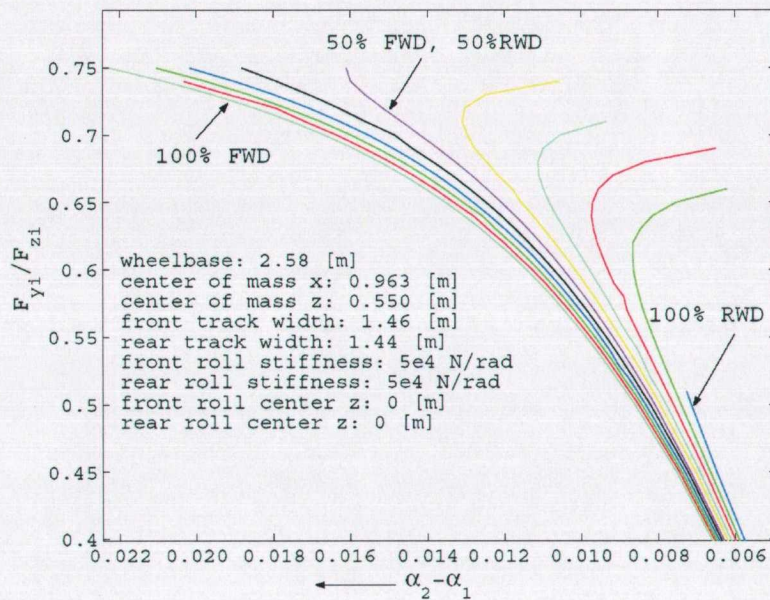

Figure 12: Handling diagram

It clearly can be seen in figure 12 that by changing the distribution of the torque needed to maintain constant speed, the vehicle dynamics can be changed from understeered to oversteered behaviour for high lateral accelerations. Note that the influence in creases with lateral acceleration or speed. Thus for very low speeds this effect will be neglectable.

This can be explained with use of the tyre characteristics. The behaviour of a tyre under combined loading conditions can be seen in figure 13. In the left plot the lateral force as a function of the side slip ngle is given for different longitudinal slip levels. In the right plot the total tyre force is given for the same load conditions.

The behaviour for large values of slip can be explained with the so called friction circle. The tyre is assumed to have the same friction coefficient for all directions. Now the direction of the force will determine the size of the lateral and longitudinal force. If a tyre experiences pure sideslip the lateral force will have the same magnitude as the friction circle. But when the tyre is also slipping longitudinal the lateral force acting on the tyre will have to be constructed from the force vector, and will obviously be smaller than the force vector see figure 14.
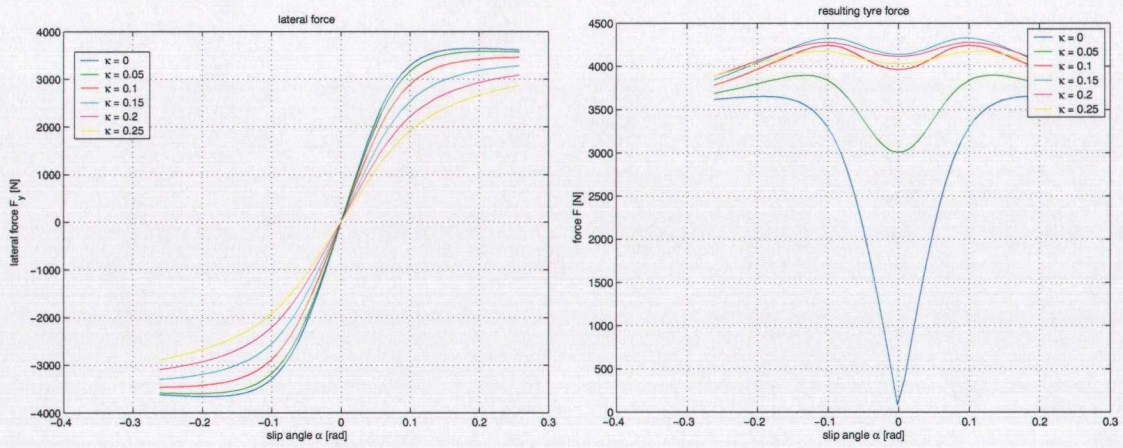
Figure 13: lateral force and resulting force
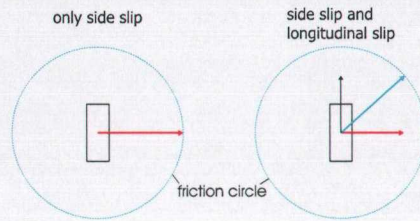
Figure 14: simple friction circle model

This theorem is based on global slip behavior. The fact that the tyre also displays this behaviour during partial slip can be explained with a simple brush tyre model see figure 15

Figure 15: Brush model [5]

In this model the tyre is considered to be a rim with a row of elastic bristles on it. When the tyre rolls the first bristle that enters the contact zone is assumed to stand perpendicular with respect to the

road surface. If the tyre is rolling freely the tread elements will remain vertical. The tread element will travel from leading edge to trailing edge without deflecting and thus without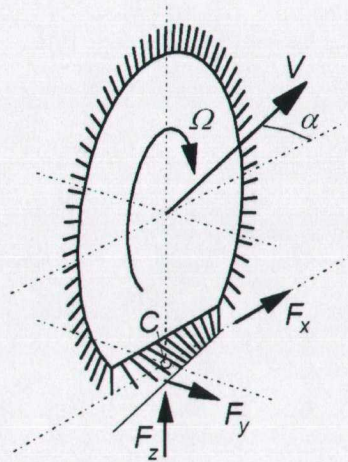 developing a lateral or longitudinal force. But if this tyre is subjected to a sideslip the bristles will deflect. The vertical force distribution is assumed to be parabolic. Then the maximum deflection of a tread element depends on its position in the contact zone. When a tread element travels through the contact zone the deflection increases linear with the position until the deflection force exceeds the local maximum see figure 16. From this point the tread element is slipping. The same yields for longitudinal slip.
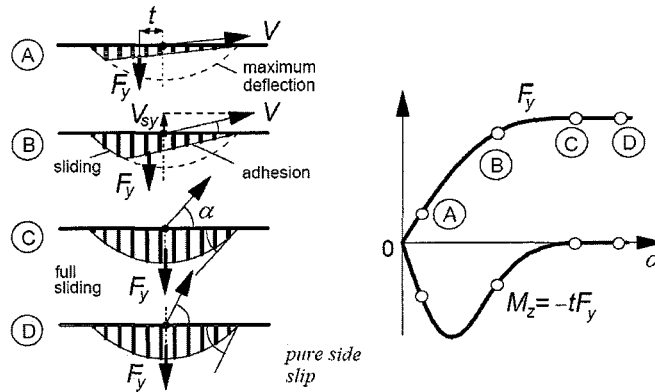

Figure 16: Bristle deflection (steady state) [5]

In the case of combined slip, the magnitude v of the deflections in lateral direction and the magnitude of the deflection in longitudinal direction u, must be summed. The total tread deflection than becomes [5]:

$$\mathbf{e} = \sqrt{u^2 + v^2} \tag{49}$$

The bristles are assumed to have an isotropic stiffness c_p and a constant friction coefficient μ. The load on the bristles per unit length is $q_z(x)$. The point of transition from adhesion to sliding region can be obtained from the condition [5]:

$$c_p|\mathbf{e}| = \mu q_z \tag{50}$$

The treads in the sliding region have reached their maximum deflection and force according to the slip circle principle. If a tyre which experiences sideslip is subjected to a drive or brake moment also longitudinal slip will occur see figure 17. Then the transition point between adhesion and sliding will move forward. In the adhesion region the lateral force remains and a extra longitudinal force is added. But for the sliding region the slip circle is applicable and here the lateral force will decrease due to the longitudinal force. This explains why there is a increase in total force but still a decrease in lateral force when a extra drive moment is applied see figure 13.

As mentioned before the vehicle maintained constant speed so the lateral force on the vehicle did not vary, only the torque distribution (no instability of the force equilibrium is assumed). Also knowing that the torque is distributed to the wheels via a differential and thus the torque on the right and left tyre are the same, it can be seen that the torque distribution influences the slip-angles of the axles and the moment about center of gravity. A front wheeldrive will have a larger slip angle at the front and will have a tendency to understeer. A rear wheeldrive vehicle will have a large slip angle at the back and will have a tendency to oversteer.

3.2 Turning behavior with E-four

To evaluate the E-four drive line possibilities a vehicle with a normal center of gravity (in this case a audi) is compared to a vehicle with a high center of gravity at the front which represents a minivan.
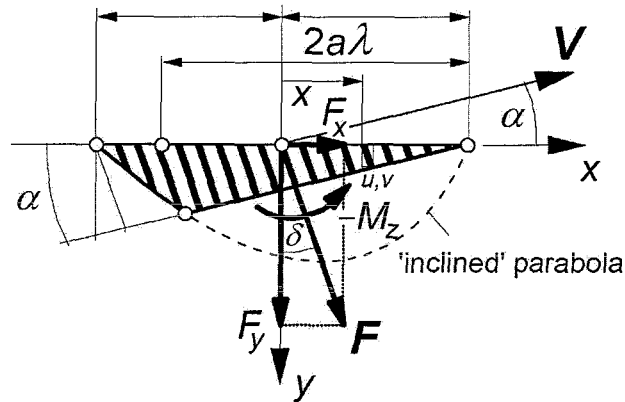
Figure 17: combined bristle deflection (steady state) [5]

Both vehicles have been modelled and subjected to a step steer at a speed of 100 km/h and a roadload of 650 N . The results can be seen in figure 18, 19 and 20. The behavior of the sedan will be different to that of the minivan. When the vehicle trajectory is plotted (initial speed is 100 km/h) it can be seen that as well the stabilization time as the final turning radius depends on the torque distribution between front and rear axle. Even some distributions are unstable for the minivan which results in extreme wheel slip and oversteered behavior. Also note that each distribution results in a different turning radius. Using the E-four drive it is possible to control the turning radius between the front wheel drive radius and the rear wheel drive radius. But the unstable situations would result in extreme tire wear. Applying the drive torque intermittingly should be investigated in order to avoid extreme tyre wear Also the transient effects could be reduced with a proper controller.

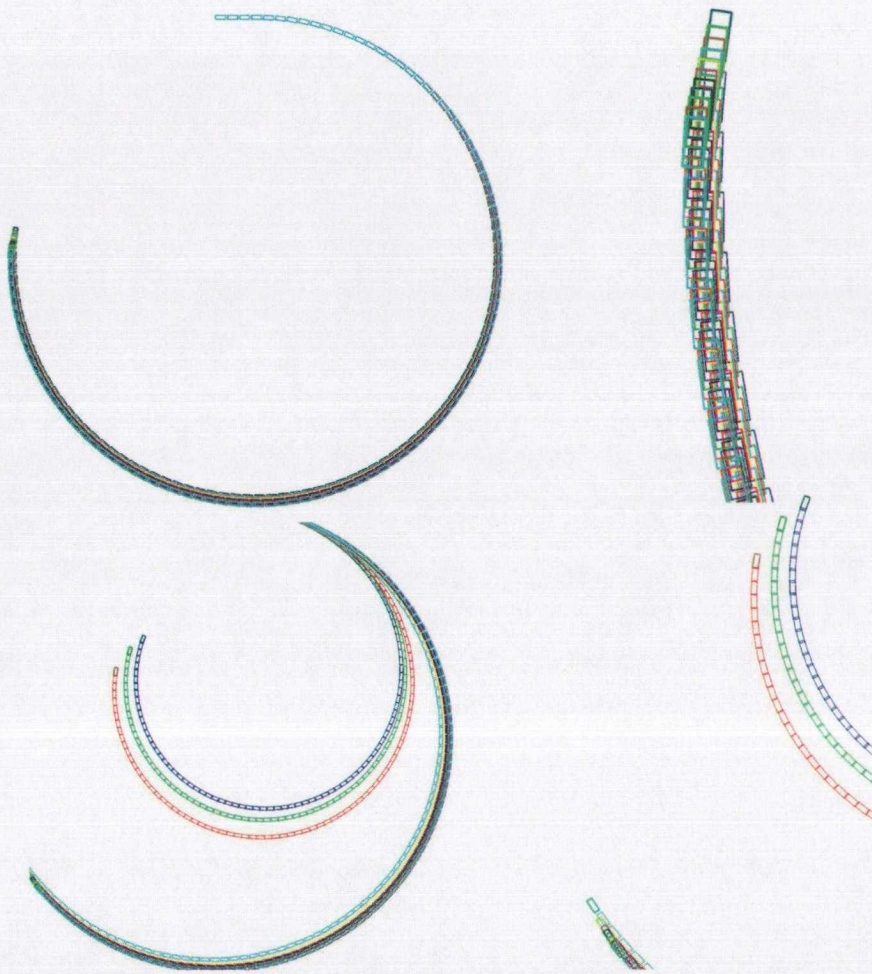The parameters used for this transient model are noted in table 3.2.

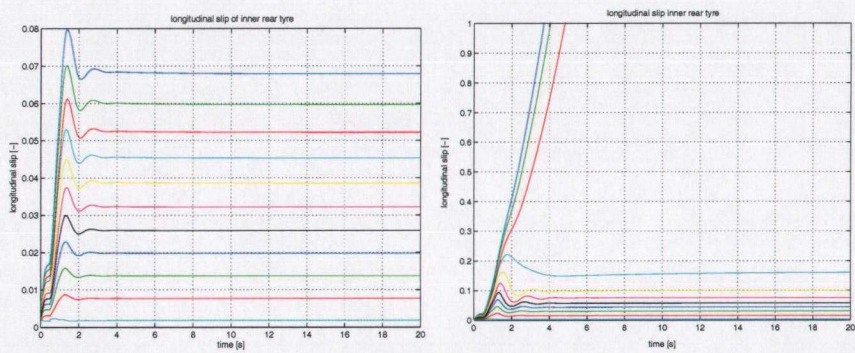Figure 18: trajectory plots: sedan (top) & minivan(bottom), right plots are zooms

Figure 19: inner rear tyre slip for sedan (left) & minivan (right)

20
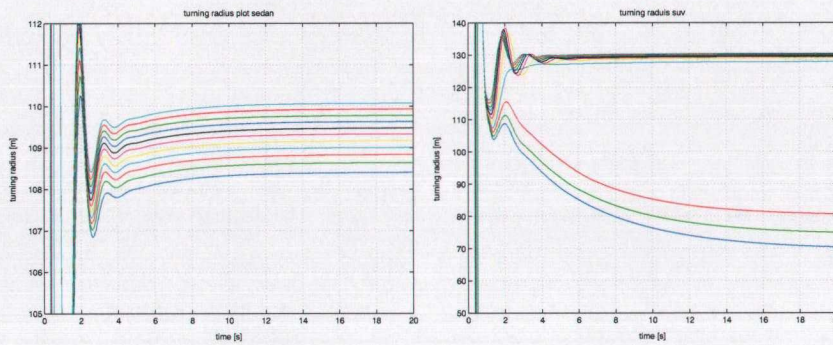
Figure 20: turning radius for sedan (left) & minivan (right)

parameter	sedan	minivan
mass	1971.8 kg	1971.8 kg
wheelbase	2.88 m	2.88 m
center of mass xcg	1.1907 m	0.95 m
center of mass hcg	0.6 m	0.85 m
Ix	900 kgm^2	900 kgm^2
Iy	3200 kgm^2	3200 kgm^2
Iz	3600 kgm^2	3600 kgm^2
Ixyz	0 kgm^2	0 kgm^2
front track width	1.591 m	1.591 m
rear track width	1.580 m	1.580 m
front roll stiffness	1.05e5 N/rad	1.05e5 N/rad
rear roll stiffness	0.55e5 N/rad	0.55e5 N/rad
front roll center height	0 m	0 m
rear roll center height	0.05 m	0.05 m
front camber	-0.6 deg	-0.6 deg
rear camber	-0.7 deg	-0.7 deg
front toe in	0.2 deg	0.2 deg
rear toe in	0.15 deg	0.15 deg
front steering compliance	0.29e-3 deg/N	0.29e-3 deg/N
rear steering compliance	0.04e-3 deg/N	0.04e-3 deg/N

Table 2: vehicle parameters sedan & minivan

4 Conclusion

The E-four drive train of the Estima was initially modeled directly into Matlab Simulink. Due to the complexity of the front drive, non-linearity of the clutches and algebraic loops to solve kinematic constraints, simulation time was unacceptably high. The model was rewritten en some kinematic constraints were eliminated. A first order state-space model is formulated for easy and efficient simulation. The designed drive mode controller ensures synchronization before closing the clutches and thus reducing clutch wear.

In order to evaluate the turning behavior of the E-four a vehicle dynamics model was constructed and used to simulate different torque distributions between front and rear axle. The influence of the torque distribution appears to be relatively small except for some unstable oversteered situations of the minivan. But when taking a closer look one can see that the final turning radius differs up to two meters for the stable situations with equal speed and steering angle. This means that after a 90 degree turn the difference between a frontwheel drive vehicle and a rearwheel drive vehicle is almost a full lane. Also the unstable situations could be used for some extreme corrections when a vehicle threatens to go off the road. Caution must be taken because of extreme tyre wear. The effectiveness of this system compared to the present ESP systems still needs to be investigated.

A Using ADVANCE

TNO recently developed a software package for vehicle simulation purposes. This package is implemented in a matlab simulink environment. In this chapter the use of advance in vehicle drive train simulations is discussed. The first subsection the view and intentions of TNO are represented. In the second subsection a assessment of the usability is given. The the drive train model of the Toyota Estima was modelled in AVANCE but due to the extensive use of algebraicloops in this model the simulation time was un acceptably long. Therefor the ADVANCE model hasn't been used for the vehicle simulations.

TNO ABOUT ADVANCE

What is ADVANCE?

ADVANCE is a vehicle model library in which the user is able to perform complete vehicle simulations [1]. Both the vehicle dynamics and the powertrain have been taken into account and may be coupled to each other. The model setup is modular, taking full advantage of the MATLAB/Simulink environment on which ADVANCE is based. This enables rapid and reusable model implementation.

The ADVANCE library, containing validated component models, is added to the Simulink libraries and may be similar to the standard libraries. The ADVANCE models have all been developed with real-time applications in mind. In addition, the user can add further models as desired. These can be tuned to the simulation requirements at hand or may be supplied by system suppliers, providing accurate behaviour based on production components.

For extra ease of use, the standard Simulink environment has been extended where needed to enable simplified handling of system parameters and post processing.

As large amounts of data are generated in the process of analysing vehicles, facilities have also been provided to reduce the load on required data storage.

Intended Usage

ADVANCE is intended to be used in the vehicle development process, from vehicle architecture studies up to detail development of real-time control systems. Some example applications are:

- Complete vehicle simulation for coupled powertrain and chassis behaviours

- Determination of fuel efficiency, optimum transmission shift strategies

- Component specification

- Powertrain architecture studies

- Control system development and prototyping, e.g. for hybrid power management, active chassis control simulation

Features

ADVANCE provides the following features [1]:

- Flexibility: Models can vary from simple (e.g. 1D powertrain simulation) to complex coupled simulation (e.g. coupled powertrain and chassis simulation, with full controller definition).

- Designed for real-time applications: modules are suitable for rapid control prototyping and hardware-in-the-loop development techniques.

- Coupling with TNO-DynaMo for detailed engine development.

- Includes the TNO MF-Tyre models and is compatible with SWIFT-Tyre high frequency tyre models via the Standard Tyre Interface.

- Component models are validated, but still flexible enough to enable modification to match requirements.

- ADVANCE provides an open architecture. One can use its own models within ADVANCE.

- Full access to all MATLAB/Simulink functionality is provided, including compatibility with all standard solvers.

- Models can be visualised in a 3D environment.

Using its cause-to-effect methodology, ADVANCE is especially suited to specification, system and control system development tasks.

usability in within AES cirriculem at TU/e

Using ADVANCE in research internships, courses and other assignments at the TU/e can have several advantages. Although the description of TNO is very promising the library is not sufficient at the moment. Most models will have to be custom made. However ADVANCE gives the opportunity to do complete (although very standard) vehicle simulations without having to model the complete vehicle oneselves. This facilitates a strict focus on the area of interest and still keep the overall picture in mind.

The system is designed in a modular way. There are empty modules available for self made models. Although it takes some time to get used to the structure used to communicate between the subsystems the system isn't to hard to get acquainted with. Using this environment the storage and plotting of results can be done in a simple manner (without the usual hassle of creating the right plot line for the desired result). An other major advantage is that the system will enforce a common programming style and thus increases the compatibility between models developed by different people.

A few things should be taken into account when modelling a system that will be incorporated in ADVANCE. First one should avoid globalized variables. Define everything local and use in/output ports to communicate with subsystems. This avoids interference in advance and gives a clearer overview of the dataflow. Further the in and output of the complete system should comply with advance standards: The inputs should be torque and accumulated inertia of the drivetrain upto that block, the output should be ω and $\dot{\omega}$ which is the feedback for the previous block. All control signals are communicated through the bus system. Also all data that should be available for postprocessing should be fed into the bus system.

Because the torque as well as the inertia are propagated forward through the system, it is possible that the dynamics are solved as one big algebraic loop instead of using a algebraic loop per component or even without loops. But no information on the exact solving method is available at the moment. This needs to be looked into further.

24

B The general case of the planetary gear

The general case of a planetary gear with three inertias and three torques applied will be considered here in more detail. See fig 21
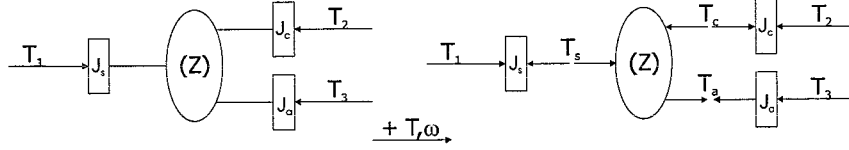

Figure 21: general case of a planetary gear

The kinematic and static equation for a double pinion planetary gear are (as mentioned previously):

$$\omega_s = (1+z) \cdot \omega_c - z \cdot \omega_a \qquad ; z = -\frac{r_a}{r_s} \tag{51}$$

$$\dot{\omega}_s = (1+z) \cdot \dot{\omega}_c - z \cdot \dot{\omega}_a \tag{52}$$

$$T_a = z \cdot T_s \tag{53}$$

$$T_c = (1+z) \cdot T_s \tag{54}$$

The equations of motion for this system are :

$$J_s \cdot \dot{\omega}_s = T_1 - T_s \tag{55}$$

$$J_c \cdot \dot{\omega}_c = T_c - T_2 \tag{56}$$

$$J_a \cdot \dot{\omega}_a = -T_a - T_3 \tag{57}$$

After rewriting and substituting the equations of motion into eqn.52 the equations become:

$$J_s \dot{\omega}_s = J_s \cdot \left((1+z) \cdot \frac{T_c - T_2}{J_c} - z \cdot \frac{-T_a - T_3}{J_a} \right) = T_1 - T_s \tag{58}$$

Now an explicit expression for T_s can be found with use of eqn. 53, 54 and 55:

$$T_1 - T_s = J_s \cdot \left((1+z) \cdot \frac{(1+z) \cdot T_s - T_2}{J_c} - z \cdot \frac{-z \cdot T_s - T_3}{J_a} \right) \tag{59}$$

$$T_s = \frac{J_a \cdot J_c \cdot T_1 + (1+z) \cdot J_a \cdot J_s \cdot T_2 - z \cdot J_c \cdot J_a \cdot T_3}{J_c \cdot J_a + J_a \cdot J_s \cdot (1+z)^2 + J_c \cdot J_s \cdot z^2} \tag{60}$$

C Lumping the CVT pulley inertias

As mentioned before the third part consists of the primary and secondary cvt pulleys. When lumping two inertias connected by a gear ratio the, the lumped inertia will depend on the gear ratio. If the ratio is time dependant like in a cvt, a extra torque will be induced when the ratio is changed with a speed of $\dot{r}(t)$ (for convenience the time dependency is not noted in the formulas). Combining the separate EOM and the kinematic relations a combined EOM can be found: (here also all intermediate steps are noted)

$$J_{prim} \cdot \dot{\omega}_{prim} = T_{prim} - T_{belt} \tag{61}$$

$$J_{sec} \cdot \dot{\omega}_{sec} = T_{sec} - T_{rd} \tag{62}$$

$$T_{rd} = (T_{kl} + T_{kr}) \cdot \frac{1}{r_d} \tag{63}$$

$$\omega_{sec} = \frac{1}{r} \cdot \omega_{prim} \tag{64}$$

$$T_{belt} = \frac{1}{r} \cdot T_{sec} \tag{65}$$

$$\dot{\omega}_{sec} = -\frac{1}{r^2} \cdot \dot{r} + \frac{1}{r} \cdot \dot{\omega}_{prim} \tag{66}$$

$$T_{belt} = \left(\frac{1}{r^2} \cdot J_{sec}\right) \cdot \left(-\frac{1}{r} \cdot \dot{r} \cdot \omega_{prim} + \dot{\omega}_{prim}\right) + \frac{1}{r} \cdot T_{rd} \tag{67}$$

$$\dot{\omega}_{prim} = \frac{T_{prim} + \frac{\dot{r} \cdot \omega_{prim} \cdot J_{sec}}{r^3} \cdot - \frac{T_{rd}}{r \cdot r_d} \cdot}{\left(J_{prim} + \left(\frac{J_{sec}}{r^2} \cdot\right)\right)} \tag{68}$$

Note that $T_{rd} = T_{kl} + T_{kr}$ and $T_{prim} = T_{C1} + T_{C2}$ In equation. 68 the term $\left(J_{prim} + \left(\frac{J_{sec}}{r^2}\right)\right)$ represents the equivalent inertia of the combined system, and $\left(\frac{\dot{r} \cdot \omega_{prim} \cdot J_2}{r^3}\right)$ represents the toque induced by the extra acceleration due to gear changing.

26

References

[1] TNO Automotive ADVANCE brochure, *http://www.automotive.tno.nl/vd/docs/brochure_advance.pdf*.

[2] Hiroatsu Endo, Masatoshi Ito, and Tatsuya Ozeki, *Development of toyota's transaxle for mini-van hybrid vehicles*, JSAE 24 (2003).

[3] G. Lechner and H. Naunheimer, *Automotive transmissions*, Springer-Verlag, 1994.

[4] Pablo Noben, *Modelling of the toyota estima mpv 2.4 16v hybrid*.

[5] Hans B. Pacejka, *Tyre and vehicle dynamics*, Butterworth-Heinemann, 2002.

[6] B.G. Vroemen, *Component control for the zero inertia powertrain*, Eindhoven University of Technology, 2001.